Science Advances

Current Issue First release papers Archive About

HOME > SCIENCE ADVANCES > VOL. 11, NO. 15 > REMOVE THE INNERMOST ATOM OF A MAGNETIC MULTI-SHELL GOLD NANOPARTICLE FOR NEAR-UNITY…

CHEMISTRY

9 April 2025

Remove the innermost atom of a magnetic multi-shell gold nanoparticle for near-unity conversion of CO_2 to CO

Guoqing Bian[1,2]†, Dong Chen[3]†, Yuping Chen[4]†, Wei Zhang[5]†, Liang Fang[1,2,6], Qing You[1,2,6], Runguo Wang[1,2,6], Wanmiao Gu[1,2,6], Yue Zhou[1,2,6], Nan Yan[1,2,6], Shengli Zhuang[1,2,6], Shiyu Ji[1,2], Meng Zhou[5], Chengming Wang[7], Lingwen Liao[1,2,6]*, Qing Tang[4]*, Jun Yang[3]*, Zhikun Wu[1,2,6]*

[1]Key laboratory of Materials Physics, Center for Excellence in Nanoscience CAS, Hefei, Anhui, P. R. China.
[2]Key laboratory of Precision and intelligent chemistry, University of Science and technology of China, Hefei, P. R. China.
[3]State Key laboratory of Mesoscience and engineering, institute of Process engineering, CAS Beijing100190, P. R. China.
[4]School of chemistry and chemical engineering, Key laboratory of chemical theory and Mechanism, chongqing University, Chongqing, P. R. China.
[5]Hefei National Research Center for Physical Sciences at the Microscale, University of Science and Technology of China, Hefei, Anhui, P. R. China.
[6]Department of Chemistry and Centre for Atomic Engineering of Advanced Materials, Anhui University, Hefei, P. R. China.
[7]Instruments' Center for Physical Science, Hefei National Research Center for Physical Sciences at the Microscale, University of Science and Technology of China

Deepak K Patel
07/06/2025

Basics of Nanoclusters

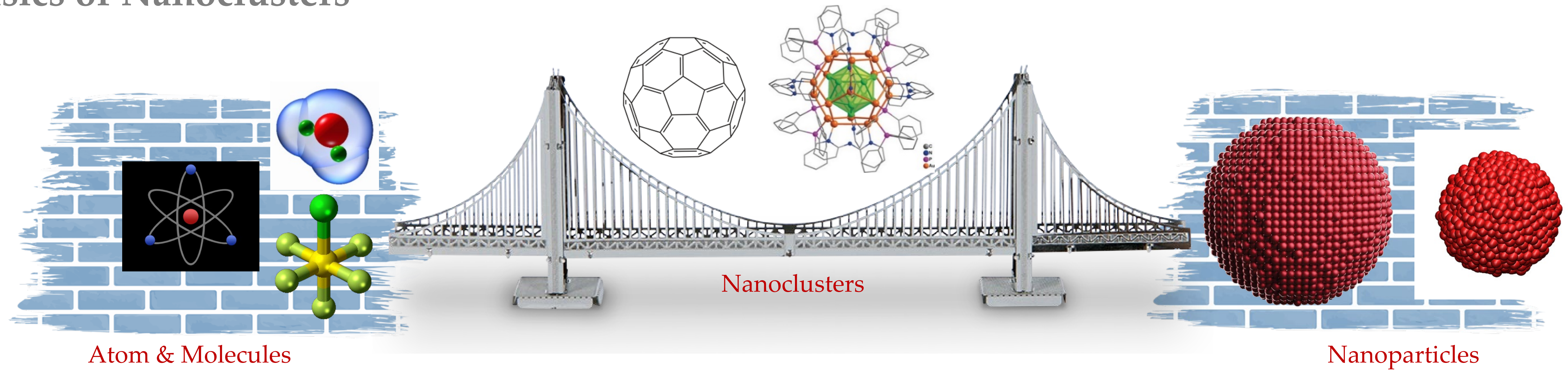

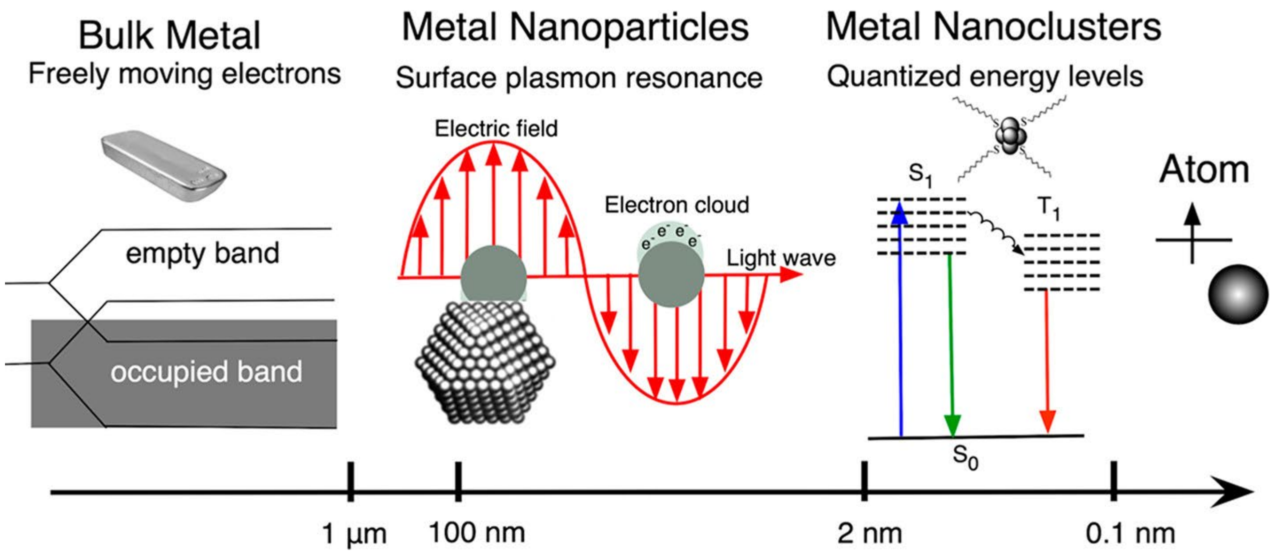

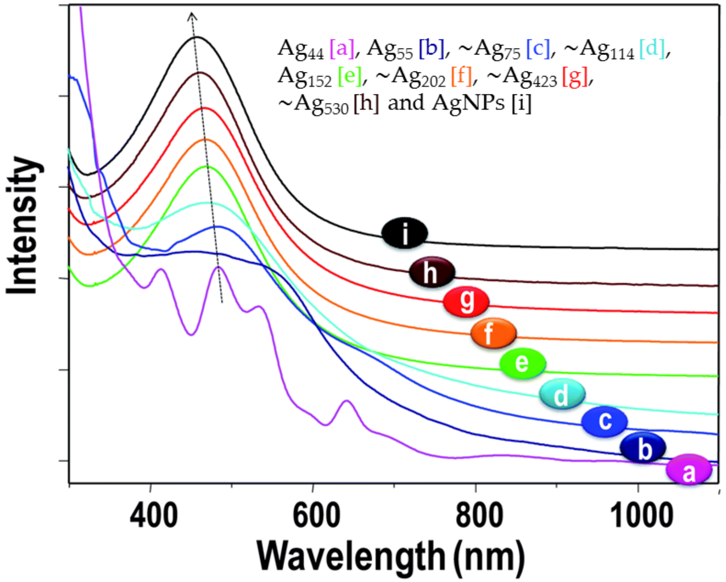

Kunwar, P. *et al.*, *ACS Appl. Nano Mater.* **2020**, 3, 8, 7325-7342

Chakraborty, I. and Pradeep, T. ***Nanoscale***, **2014**, *6*, 8024-8031

Butterfly effect, idea in chaos theory that describes how small changes to a complex system’s initial conditions can produce dramatically different outcomes.

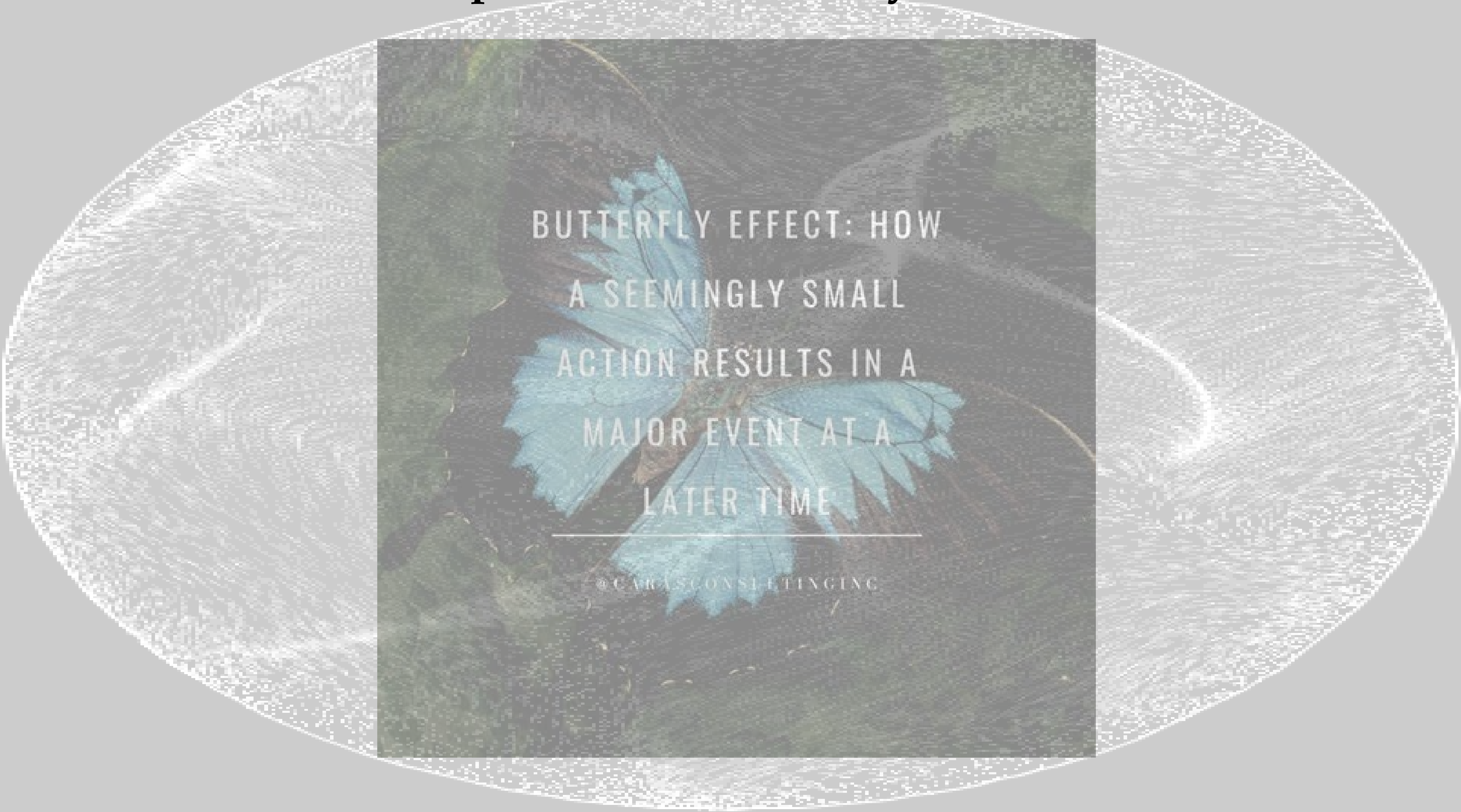

Source: Internet

Significance

Atomic-level tailoring: Demonstrates that the removal of a single core atom in a large nanocluster can switch both magnetism and catalytic selectivity.

Spin–catalysis correlation: Establishes that the absence of an unpaired spin (diamagnetism) enhances selectivity for CO_2 reduction to CO.

Surface ligand effect: Shows that spin density can be tuned by surface ligands (iodine vs. sulfur), which may influence catalysis.

Concept

Transformation from Au_{127} to Au_{126} and final $[Au_{126}]^+$

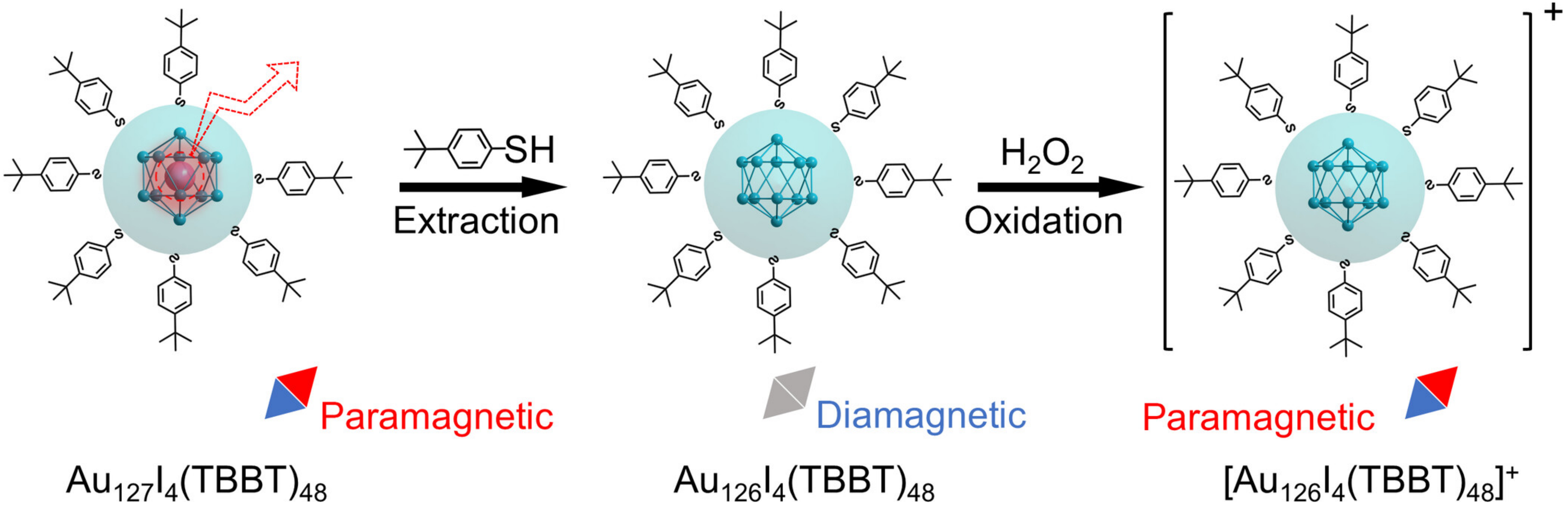

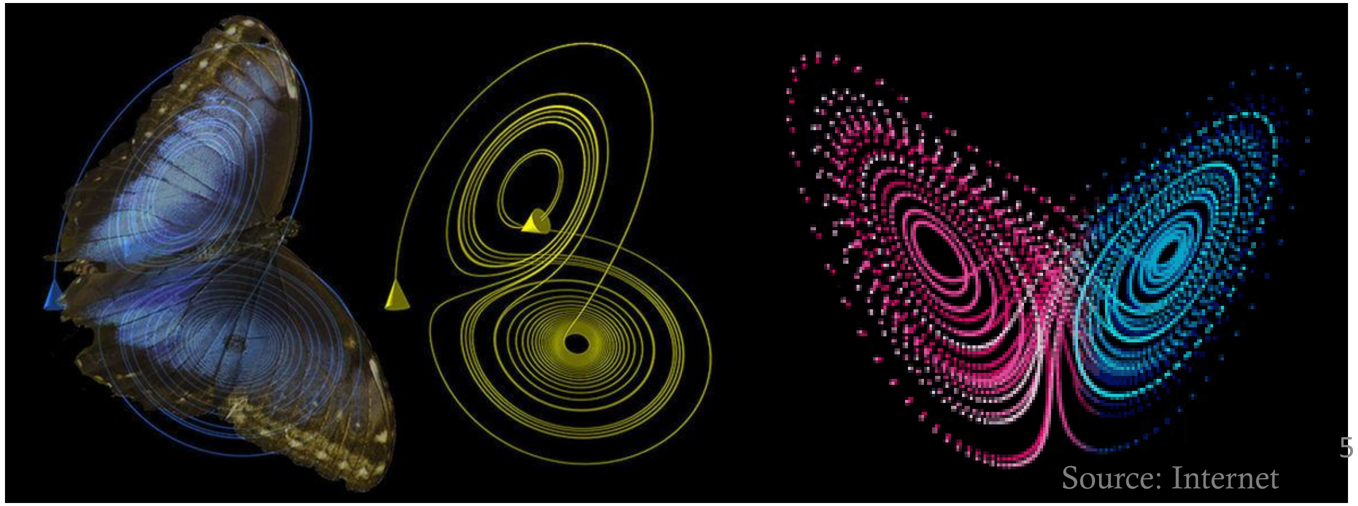

Background

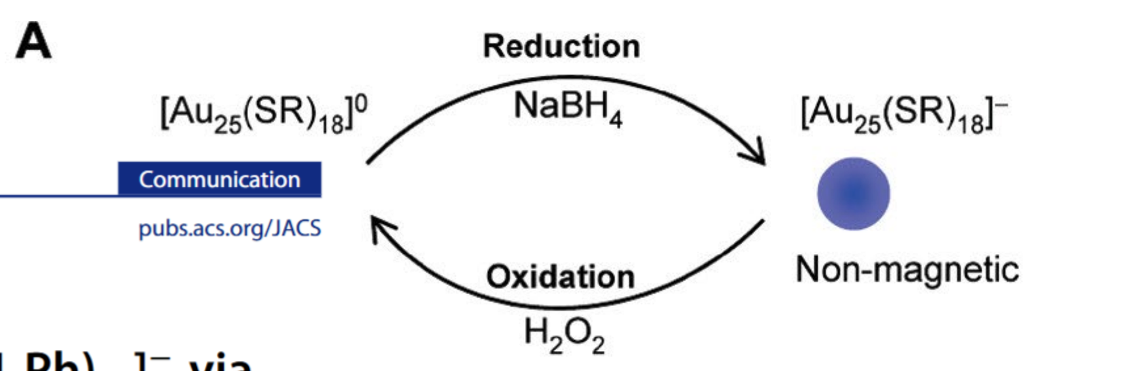

JACS JOURNAL OF THE AMERICAN CHEMICAL SOCIETY
Communication
Cite This: J. Am. Chem. Soc. 2019, 141, 14048−14051
pubs.acs.org/JACS

Stoichiometric Formation of Open-Shell $[PtAu_{24}(SC_2H_4Ph)_{18}]^-$ via Spontaneous Electron Proportionation between $[PtAu_{24}(SC_2H_4Ph)_{18}]^{2-}$ and $[PtAu_{24}(SC_2H_4Ph)_{18}]^0$

Megumi Suyama,[†] Shinjiro Takano,[†] Toshikazu Nakamura,[‡] and Tatsuya Tsukuda*[,†,§]

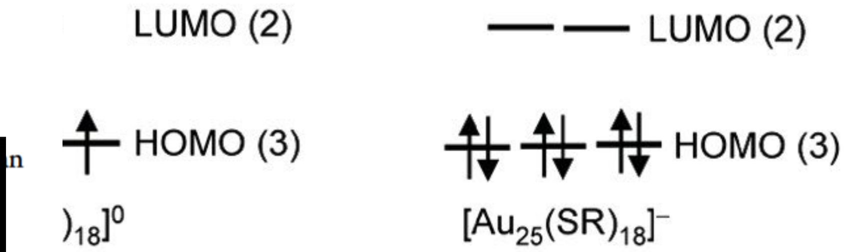

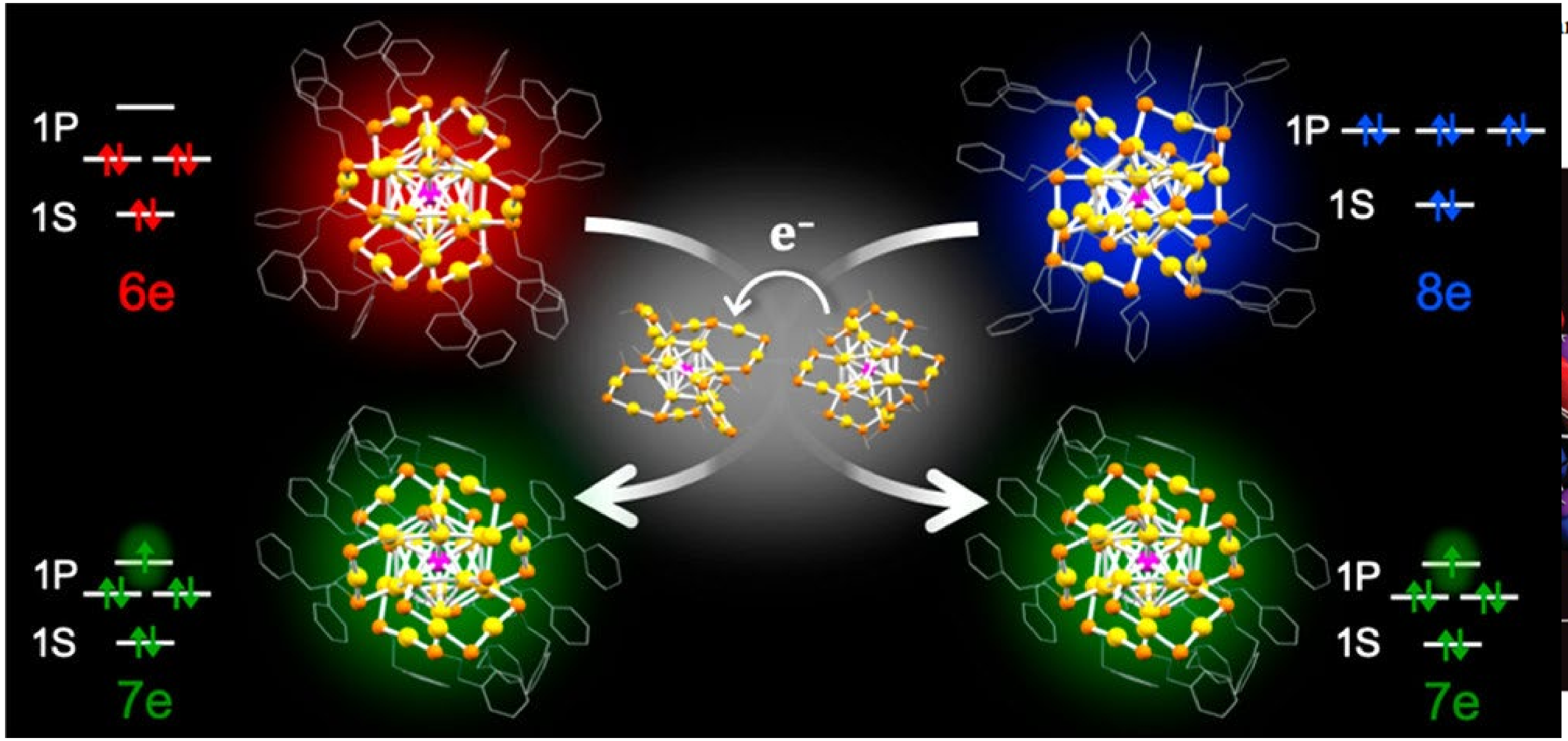

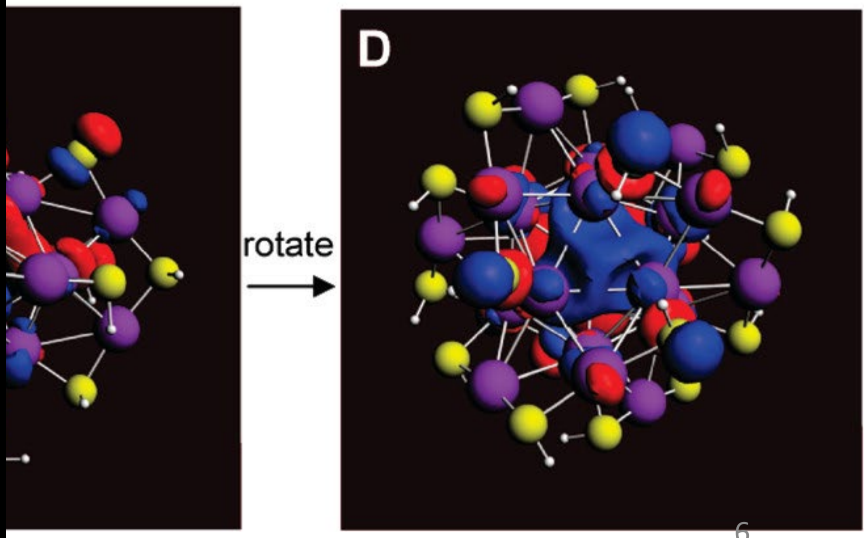

Background

Science Advances

Current Issue First release papers Archive About

HOME > SCIENCE ADVANCES > VOL. 3, NO. 5 > MOLECULAR "SURGERY" ON A 23-GOLD-

RESEARCH ARTICLE | PHYSICAL SCIENCES

Molecular "surgery" on a 23-gol

QI LI, TIAN-YI LUO, MICHAEL G. TAYLOR, SHUXIN WANG, XIAOFAN ZHU, YONGBO SONG, GIA

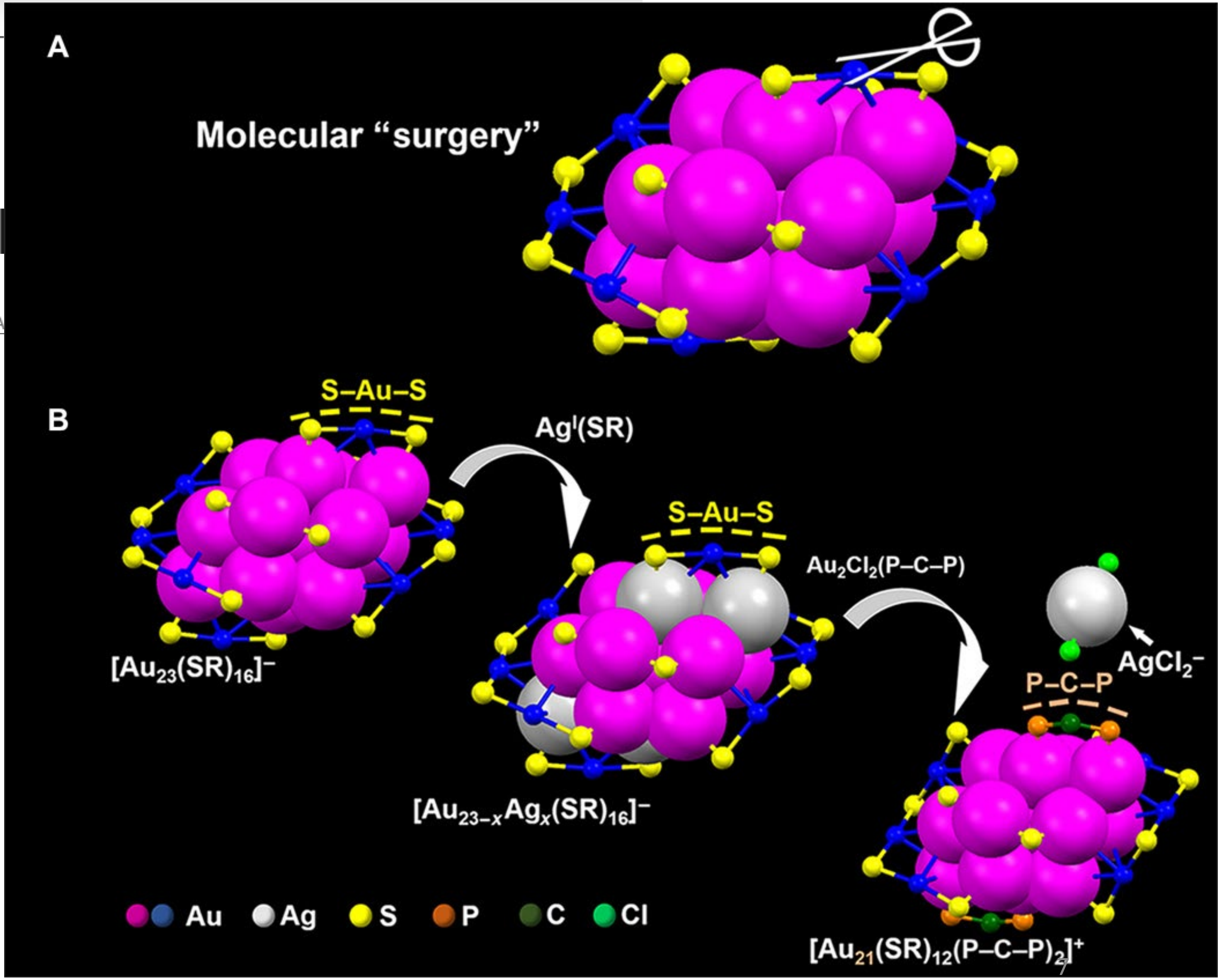

Objective:

What happens to magnetism and catalytic performance if a single atom, especially the innermost one, is removed from a large, multi-shell gold nanoparticle?

How does the spin state of such clusters influence their catalytic selectivity?

Synthesis

Synthesis Steps for Au_{127} Nanoclusters

Mix precursors in methanol

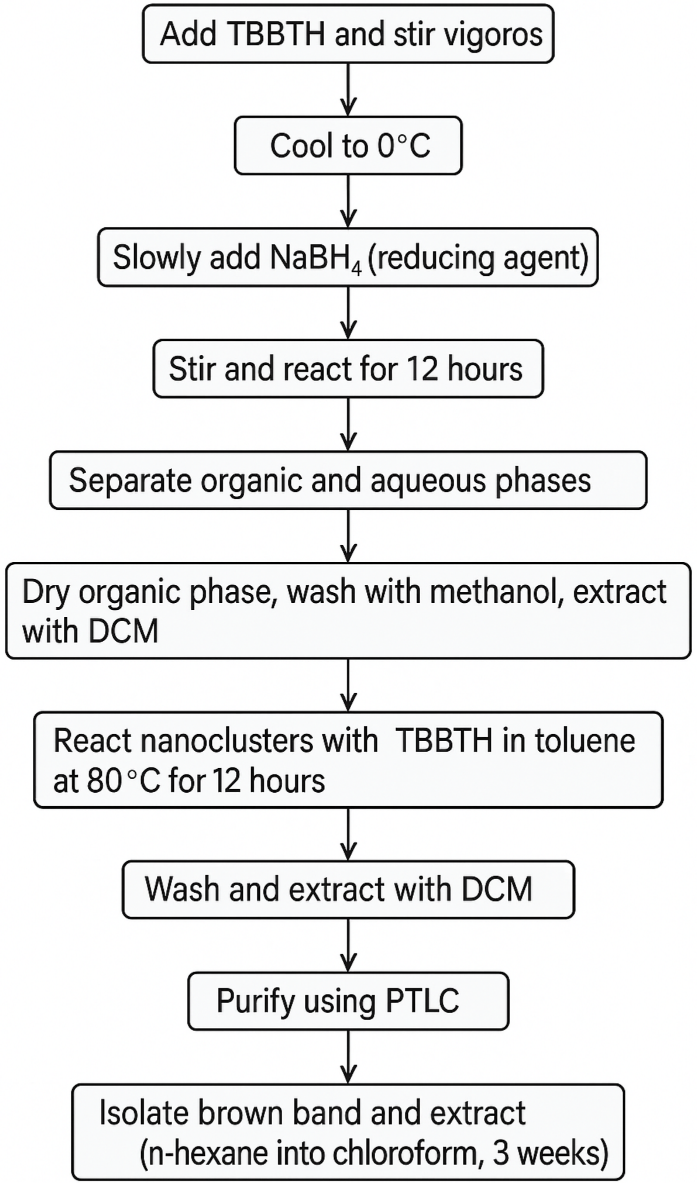

Removal of the innermost gold atom and conversion of Au_{127} to Au_{126}

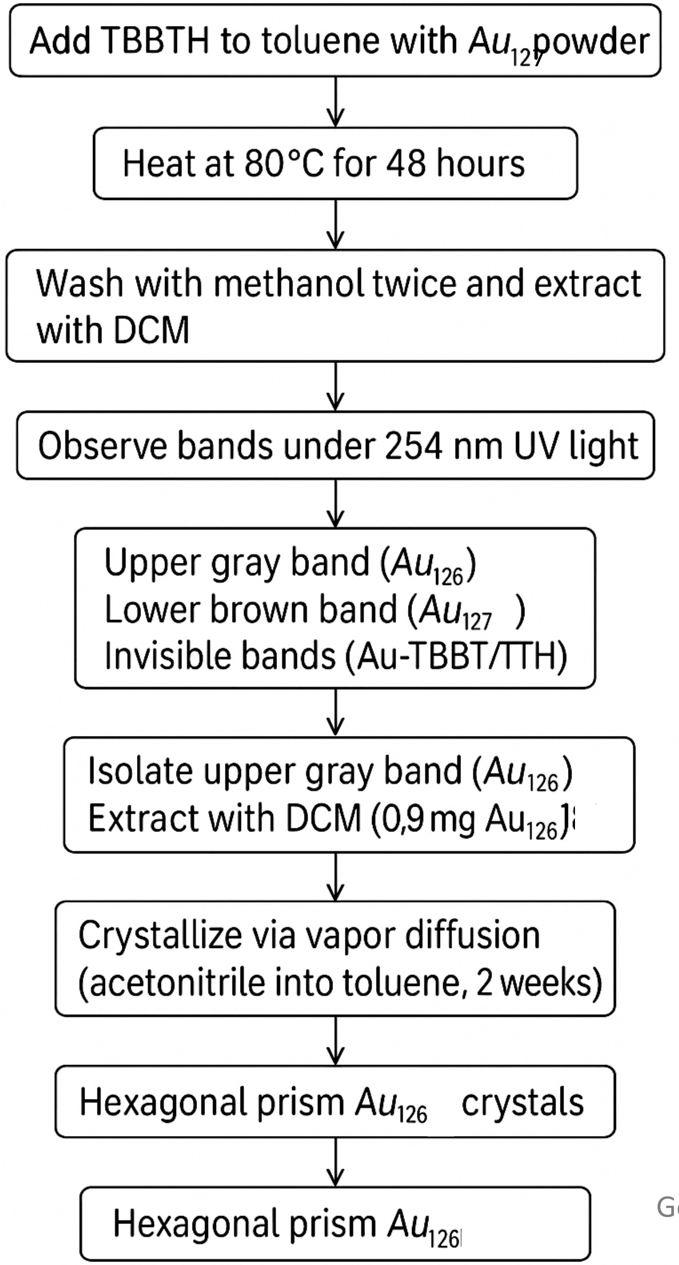

Generated using Perplexity

Synthesis

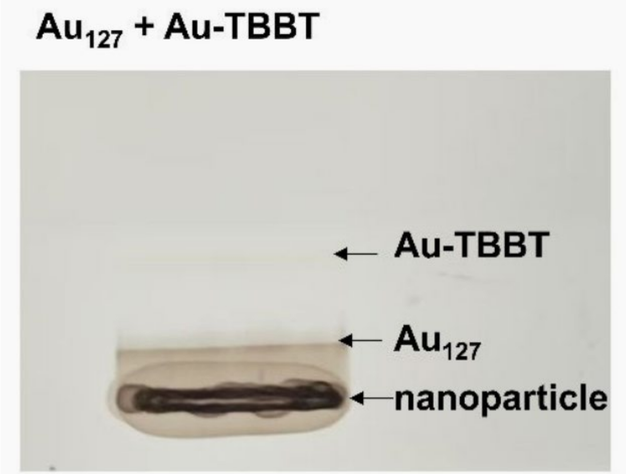

Fig. S1. PTLC monitoring of Au 127 conversion to Au126 by using quasi- antigalvanic method.

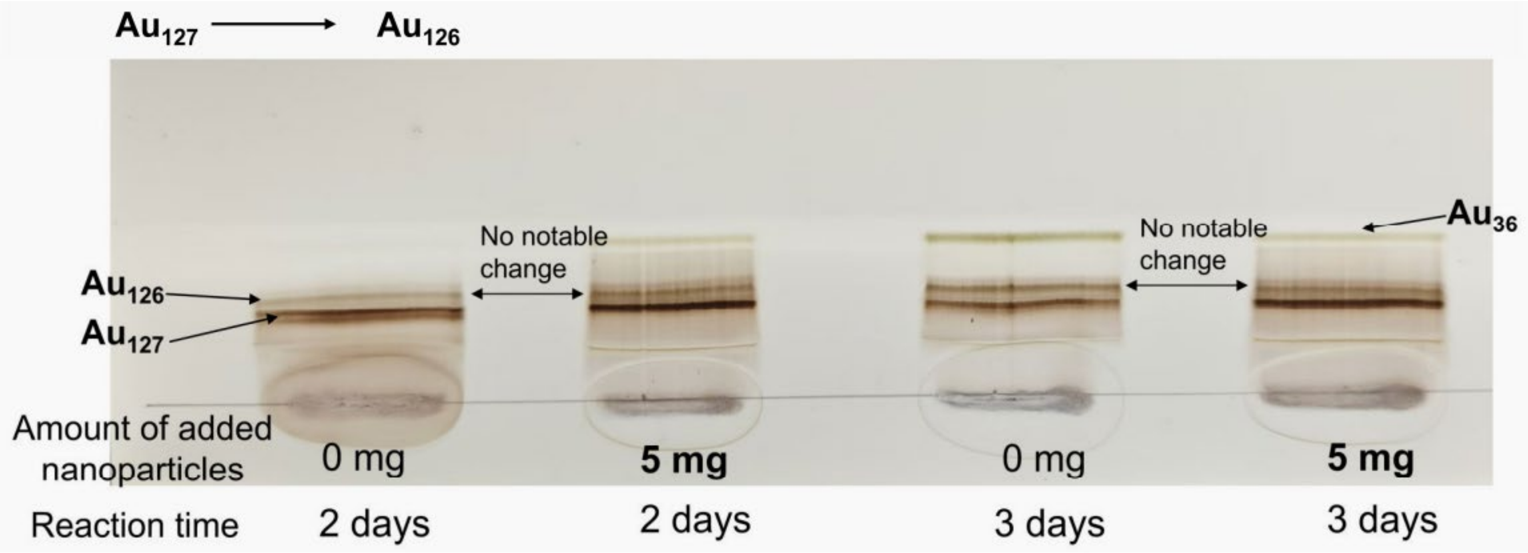

Fig. S3. PTLC monitoring of Au127 conversion to Au126 without or with the isolated relatively large nanoparticles.

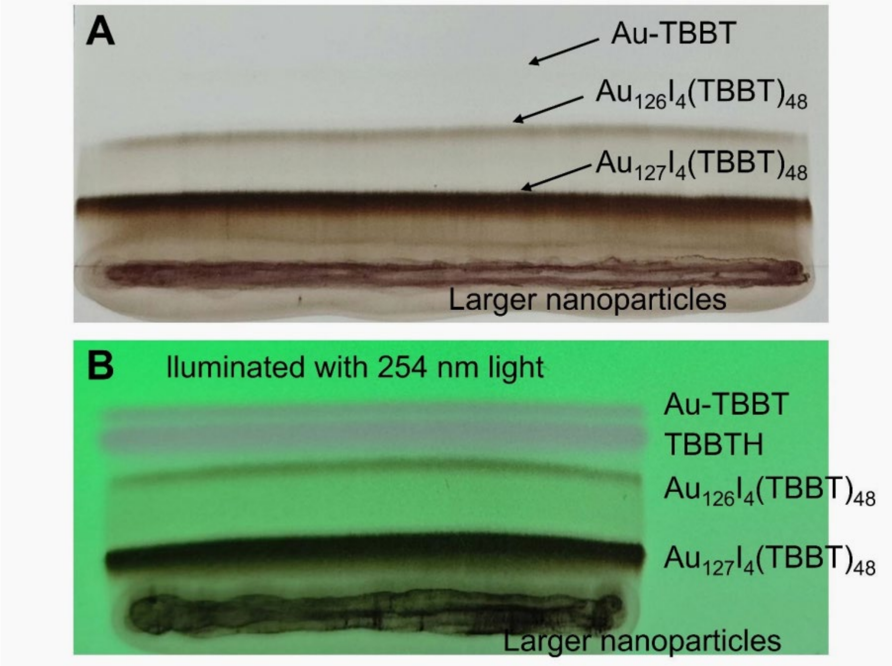

Fig. S2. PTLC monitoring of Au 127I4(TBBT)48 conversion to Au126I4(TBBT)48 without (A) or with (B) 254 nm light illumination.

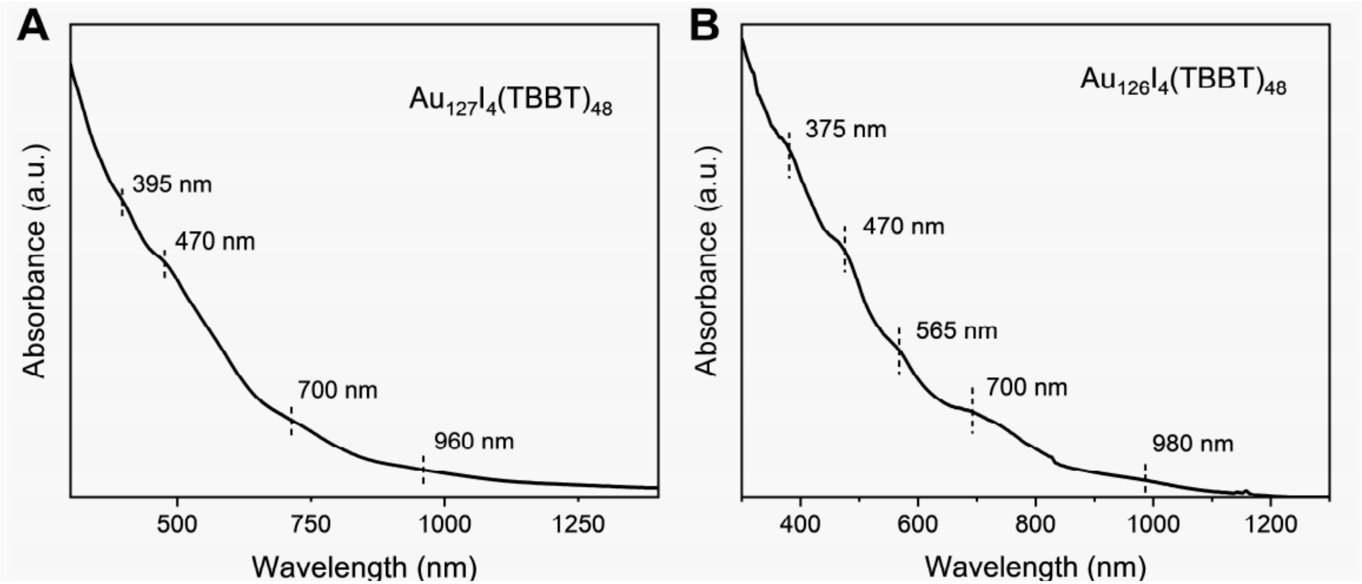

Fig. S5. UV/vis/NIR absorption spectra of Au127I4(TBBT)48 (A) and Au126I4(TBBT)48 (B) nanoclusters in toluene.

$Au_{127}I_4(TBBT)_{48}$+ TBBTH $\rightarrow Au_{126}I_4(TBBT)_{48}$ + Au-TBBT

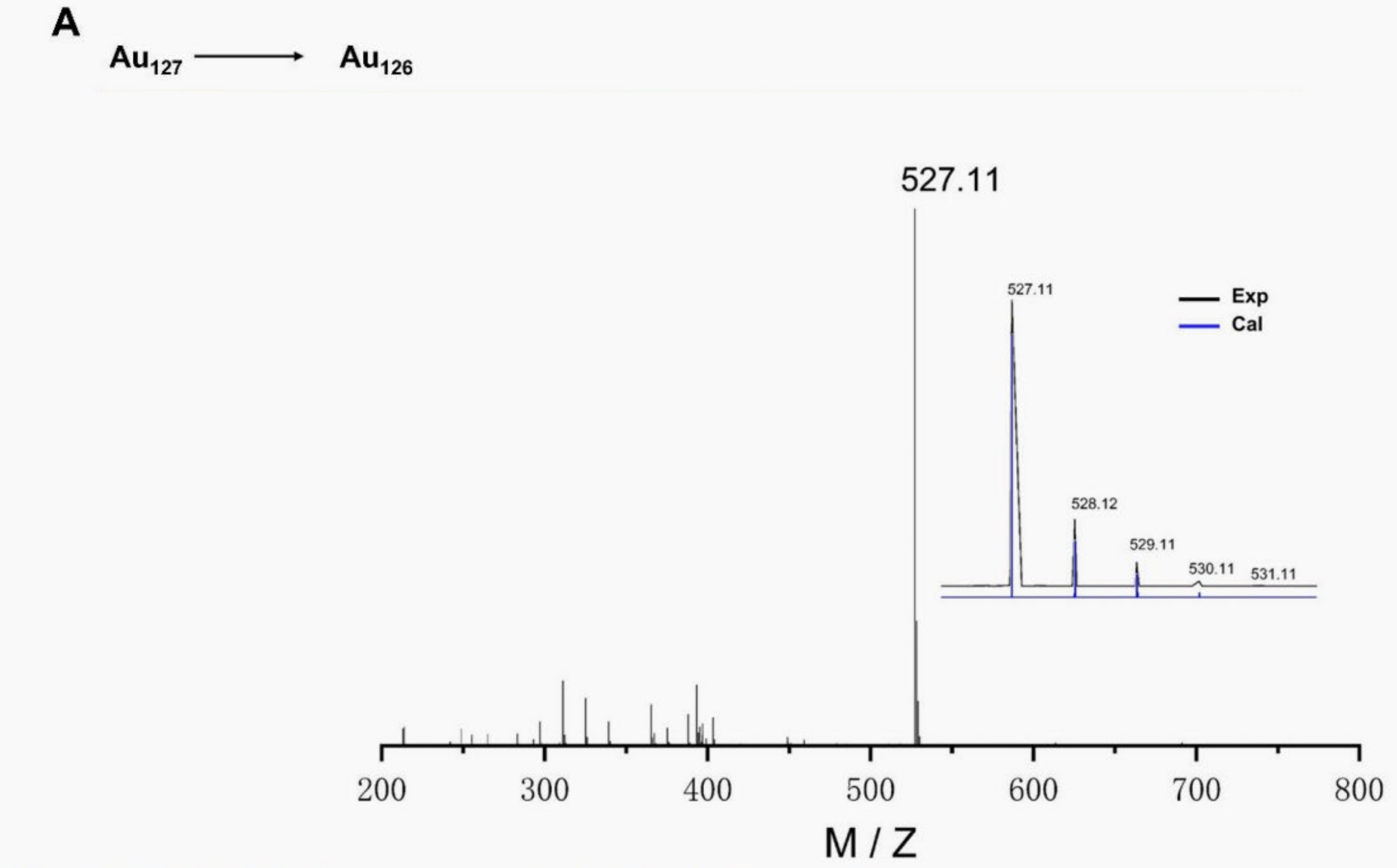

Fig. S4. ESI-MS spectrum of Au-TBBT complex.

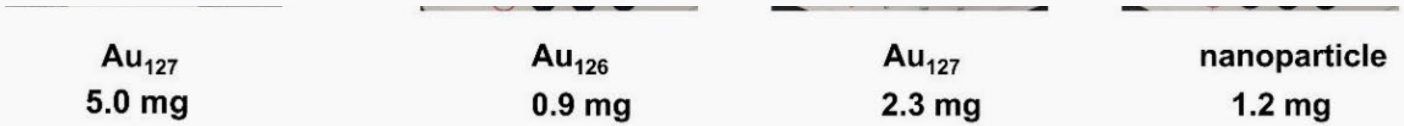

Fig. S36. PTLC monitors the time-dependent conversion (A) and the balance shows the final conversion yield (B).

Crystal system: Monoclinic
Space group: P 1 21/n 1

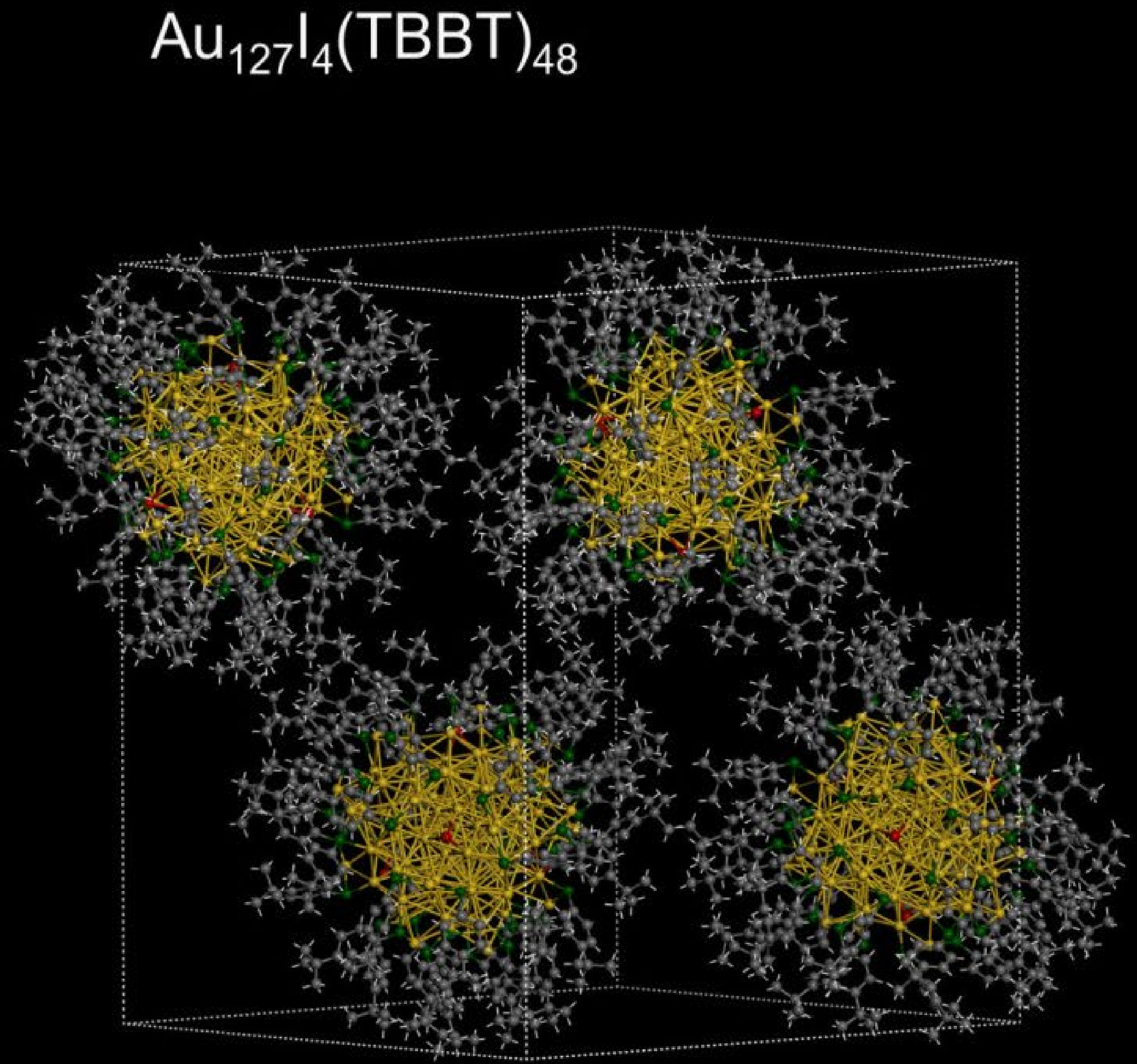

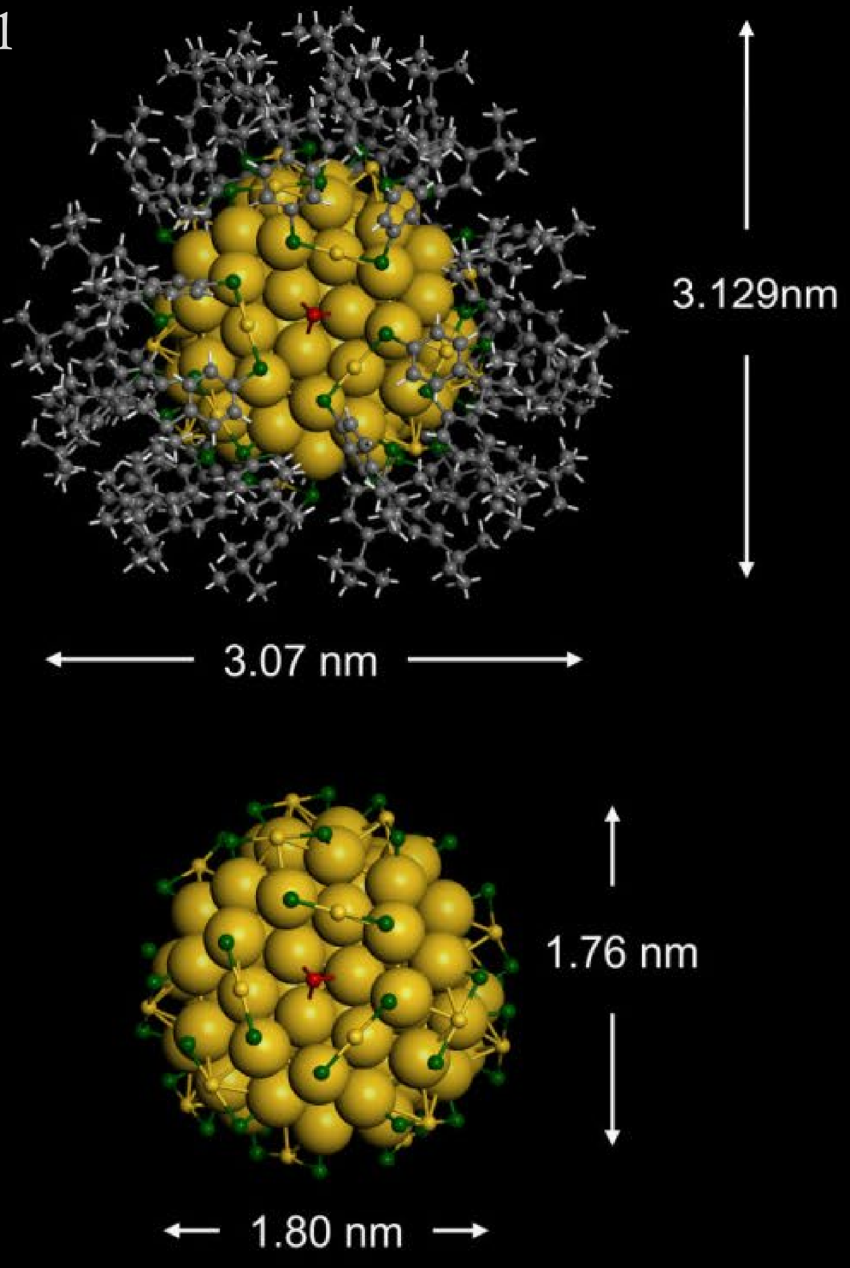

Crystal system: Trigonal
Space group: P -3

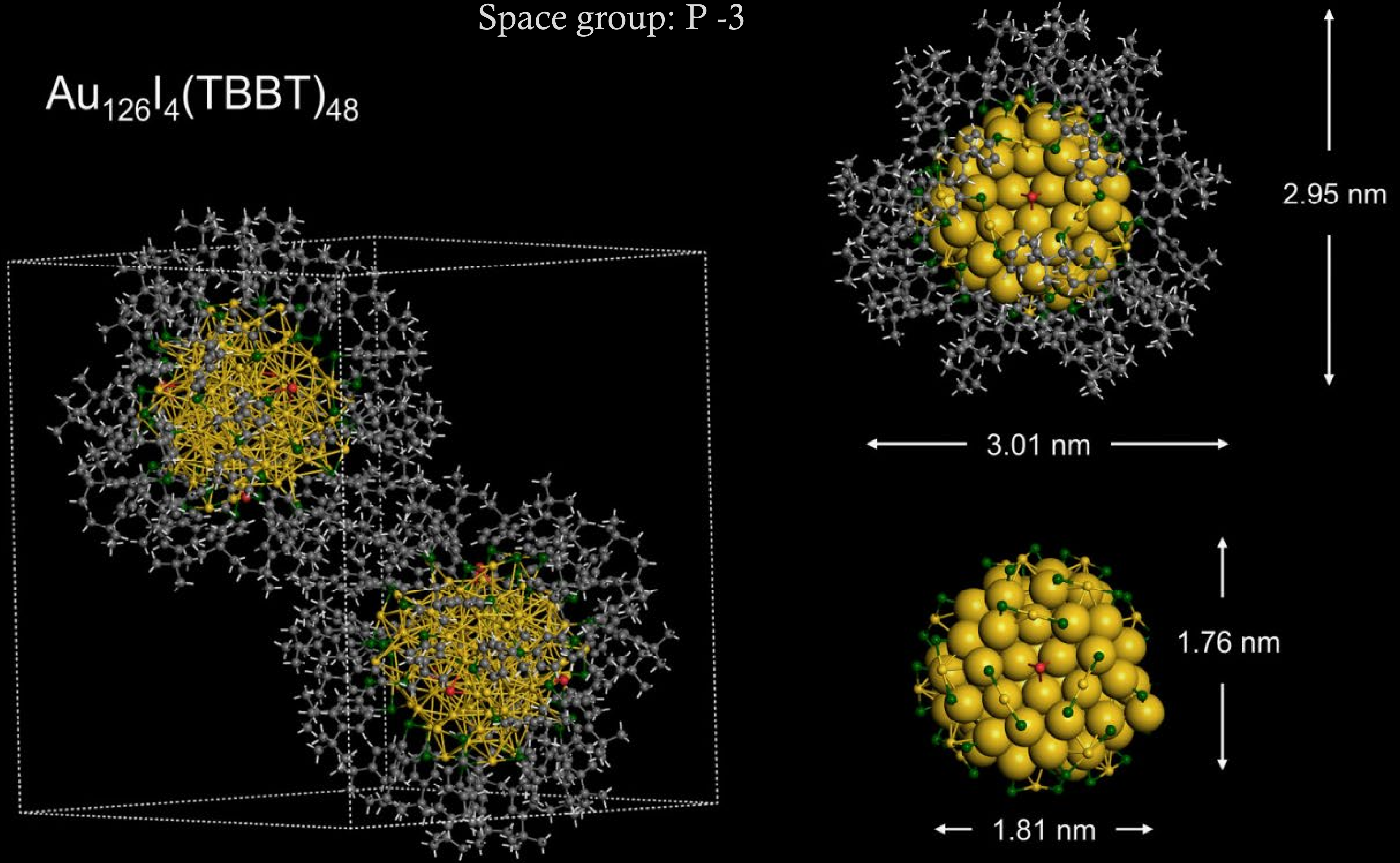

Structural Anatomy

$[Au_{13}@Au_{42}@Au_{48}I_4@Au_{24}(SR)_{48}$

Au_{13} icosahedron encapsulated within an Au_{42} icosahedral shell, forming an Au_{55} Mackay icosahedral core

The innermost Au atom removal did not alter the framework of the mother nanocluster but altered the local ligand arrangement (butterfly effect) with the elimination of paramagnetism

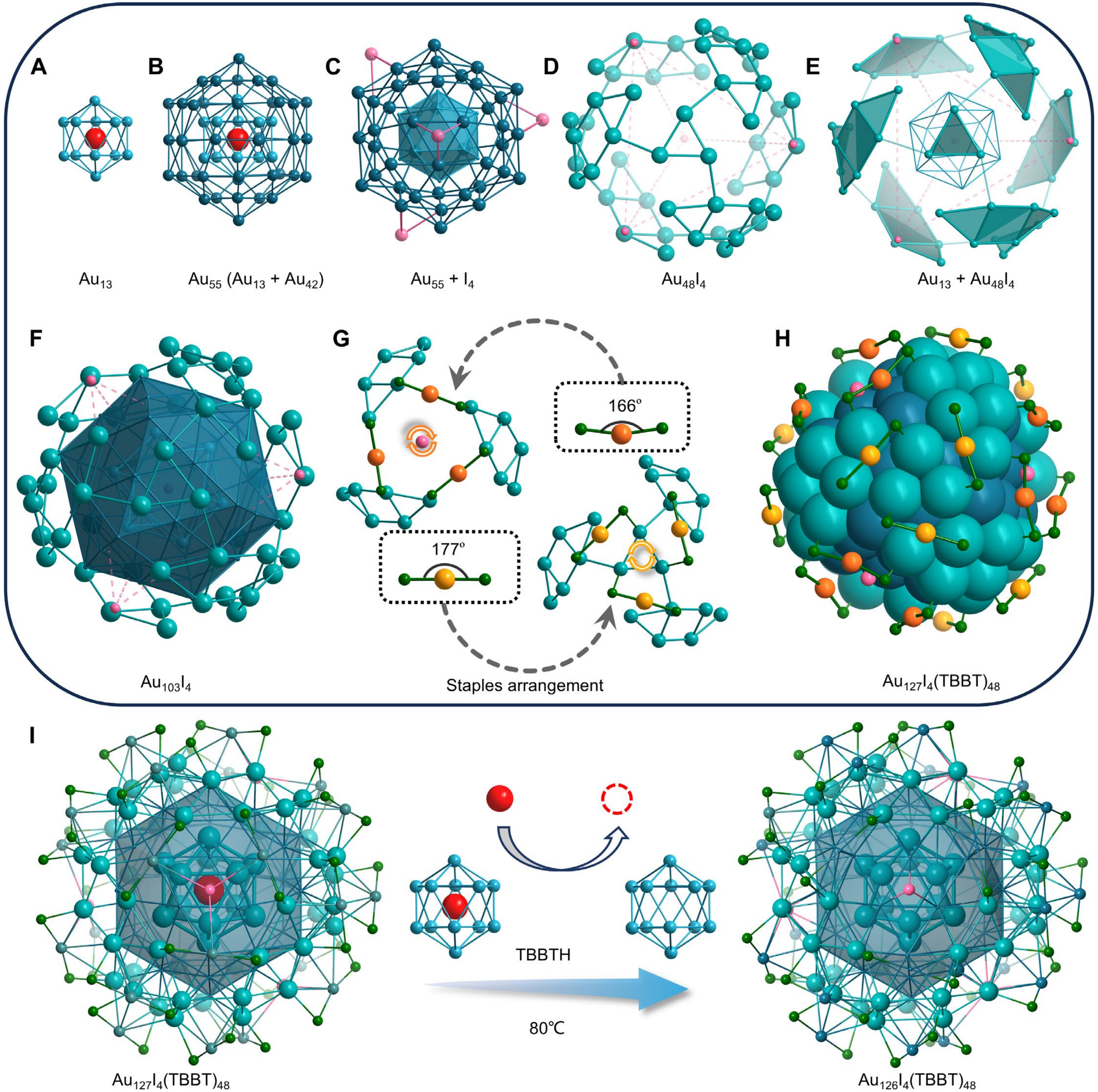

Fig. 2. X-ray crystallographic structure of Au126I4(TBBT)48 and Au127I4(TBBT)48 nanoclusters. (A) Au13 icosahedral core of Au127. (B) Au55 icosahedral core of Au127. (C) Four iodine atoms covering the four *C*3 axes of the double-layered icosahedron. (D) Au48I4 shell formed by four triangles, six spikes, and an iodine tetrahedron. (E) The Au48I4 wrapping the inner Au13 icosahedron. (F) Au48I4 reduces the core symmetry to *C*3 by wrapping the two icosahedral shells of Au127. (G) Each I atom is surrounded by three bending staples, and each Au3 triangle is surrounded by three straight staples. (H) Total structure of Au127I4(SR)48. (I) Removal of the innermost gold atom in Au127 and the transformation to Au126. The color designations are as follows: I atoms, pink; S atoms, green; Au atoms, remaining colors.

Surface monolayer assembly

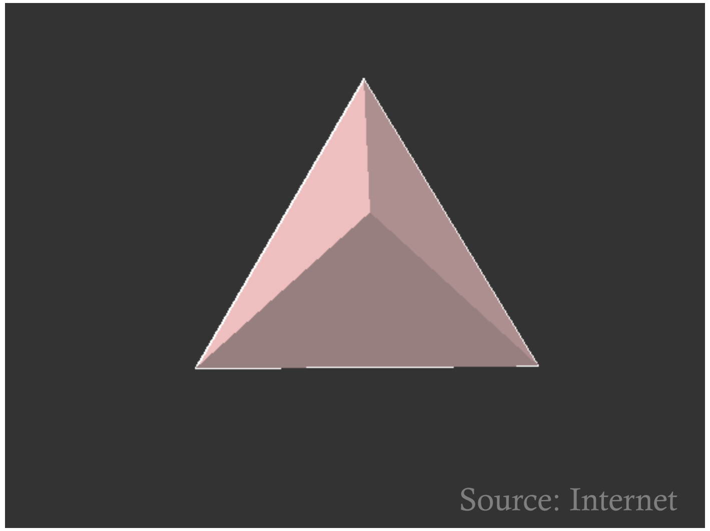

The impact of the innermost Au atom on the outermost surface ligand arrangement resembles the butterfly effect

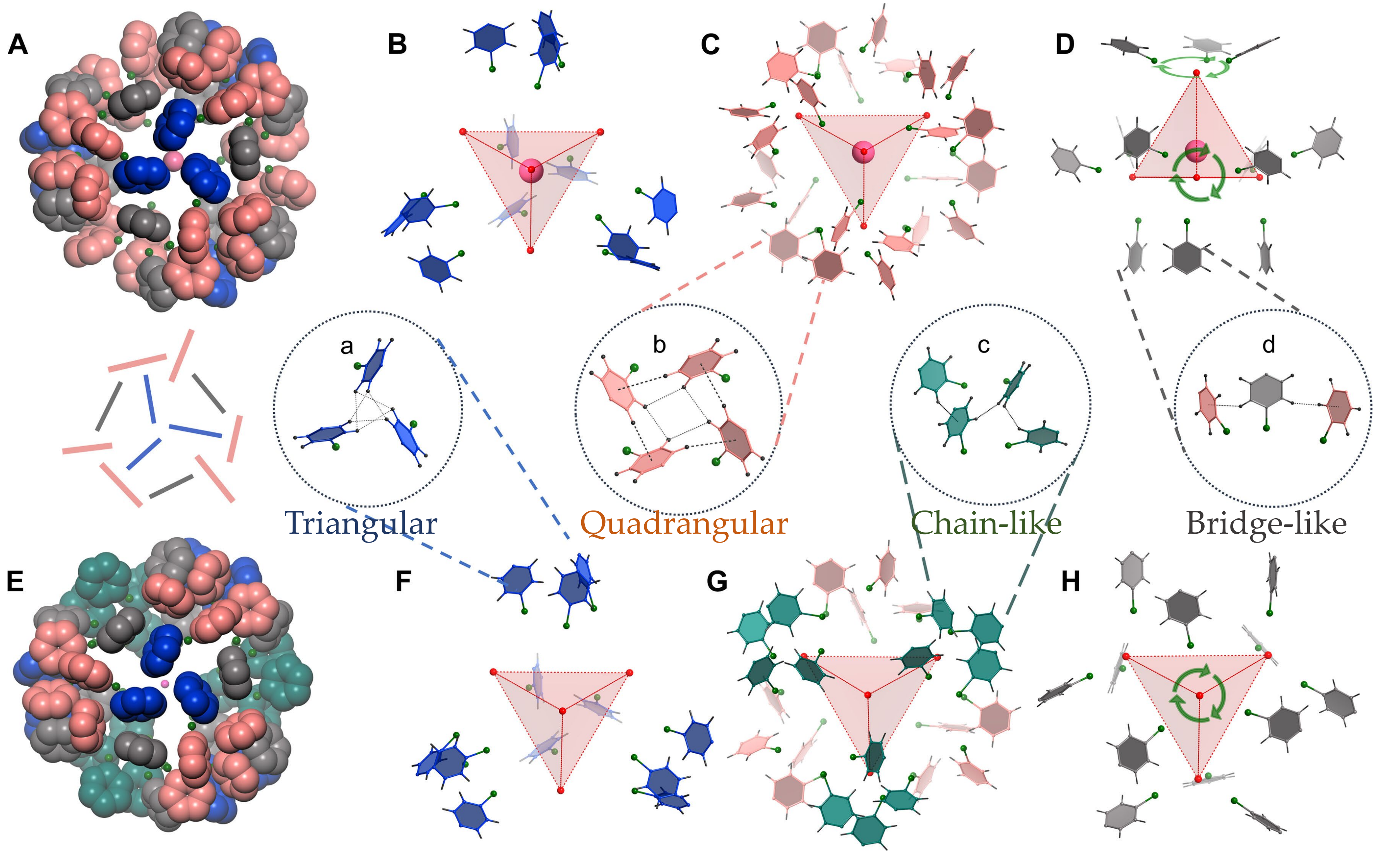

Fig. 3. TBBT and I4 monolayer on Au126 and Au127 (for clarification all tert-butyl were omitted).
The top row (A to D) illustrates the surface assembly on the Au127, and the bottom row (E to H) illustrates the surface assembly on the Au126. (A and E) Thiolate monolayer assembly on the Au127 and Au126 nanoclusters, respectively, viewed along the C3 axis. (B and F) The type-a arrangements (blue) of 12 TBBT of Au127 and Au126 are identical, distributed over the four facets of the iodine tetrahedron with each facet having three thiolates. (C) Type-b arrangement (light red) of 24 TBBT distributed on the six edges of the iodine tetrahedron with each edge having four thiolates. (G) Type-b arrangement (pink) of 12 TBBT and type-c arrangement (cyan) of 12 TBBT distributed on the six edges of the iodine tetrahedron with each edge having four thiolates. (D and H) The type-d arrangements (gray) of 12 TBBT of Au127 and Au126 are identical, distributed on the four vertices of the iodine tetrahedron with each vertex having three thiolates. The color designations are as follows: I atoms, red; central Au atom, pink; H atoms, black; C atoms, remaining colors.

Plausible transformation from Au_{127} to Au_{126} and final $[Au_{126}]^+$

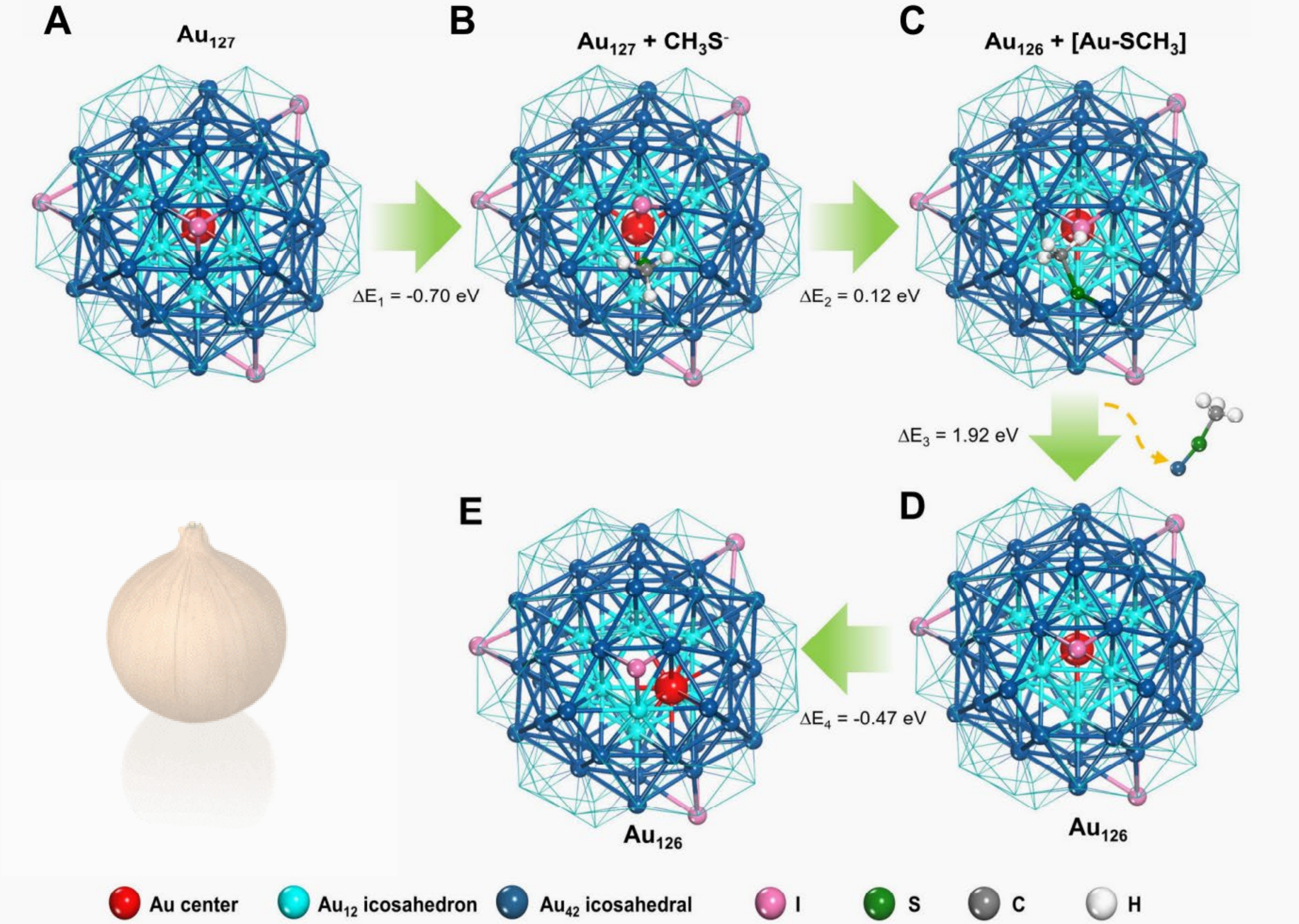

Fig. S18. A plausible transformation path proposed for DFT calculations. (A) The initial Au127 structure. (B) The adsorption of the CH3S- thiolate on one iodine-linked Au42 icosahedral Au atom. (C) The stripping of one iodine-linked Au42 icosahedral Au atom. (D) An Au atom vacancy is left in the Au42 icosahedron with the leave of Au-SCH3. (E) The final structure of Au126 after reorganization. DFT results show ΔE1 = -0.70 eV, ΔE2 = 0.12 eV, ΔE3 = 1.92 eV and ΔE4 = -0.47eV, which are accessible in our reaction conditions (ref.34 and ref. 62). The color designations are defined as follows: I atoms, pink; S atoms, green; C atoms, grey; H atoms, white; Au atoms, remaining colors. For clarification, the C, H and S atoms of the Au127 nanocluster have been omitted and the Au48 shell wrapped around the icosahedron has been shown in cyan frame. Note that, the iodine-linked Au42 icosahedral Au atom is the most likely site attacked by CH3S- among the three possible different symmetrical sites based on DFT calculations (for the other two cases, see Figure S19). To save the calculation cost, the TBBT thiolates are replaced with CH3S- thiolates.

Spin properties

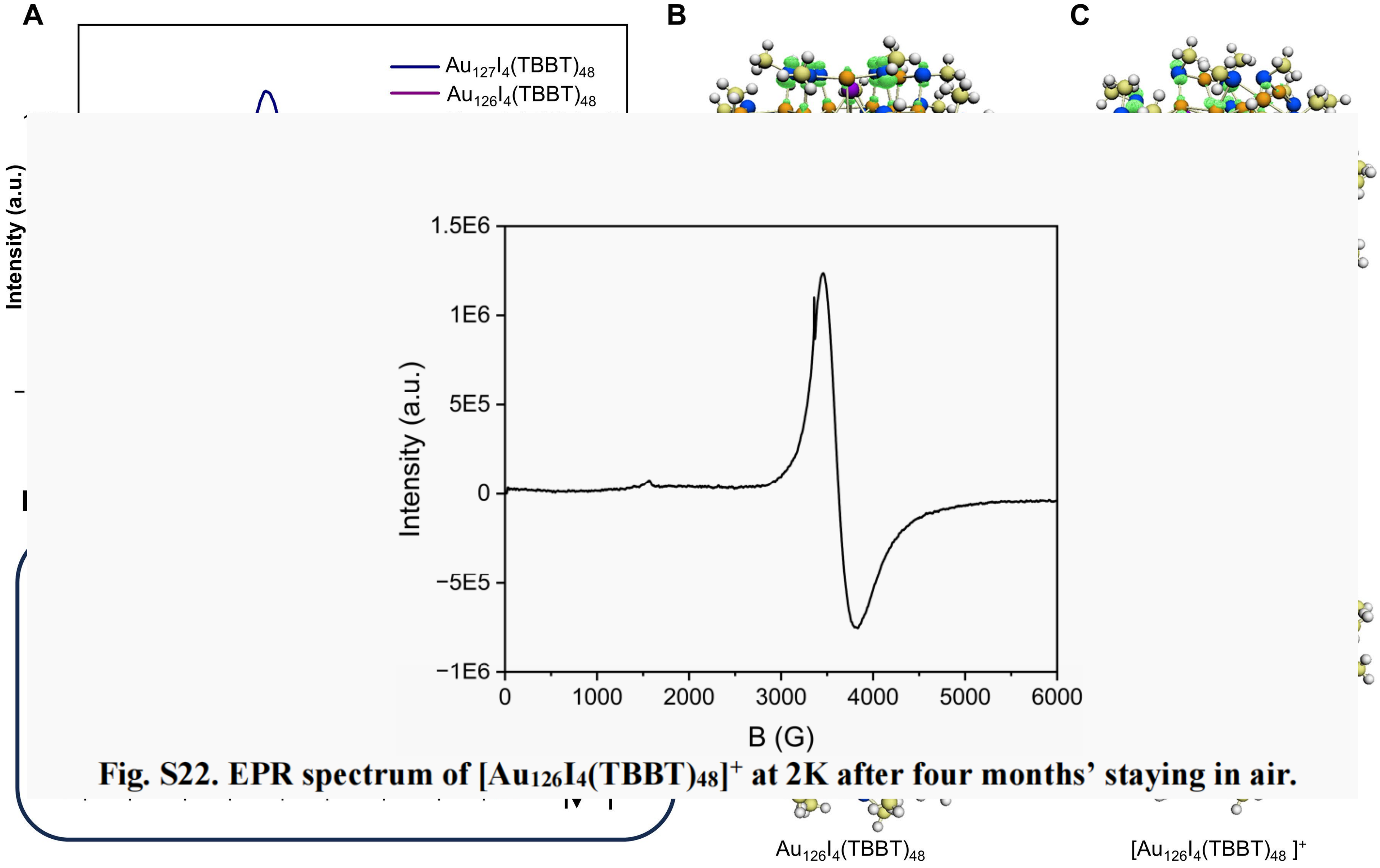

Fig. S22. EPR spectrum of $[Au_{126}I_4(TBBT)_{48}]^+$ at 2K after four months' staying in air.

Fig. 4. Spin performance of [Au126]+, Au126, and Au127.
(A) EPR spectra of Au126, [Au126]+, and Au127 powder. (B and C) Spin density distribution of Au127I4(SCH3)48. (D) Superatom orbital arrangements of the valence electrons of Au126, [Au126]+, and Au127. (E) Spin density distribution of Au126. (F) Spin density distribution of [Au126]+. a.u., arbitrary unit.

Electrocatalytic CO_2RR

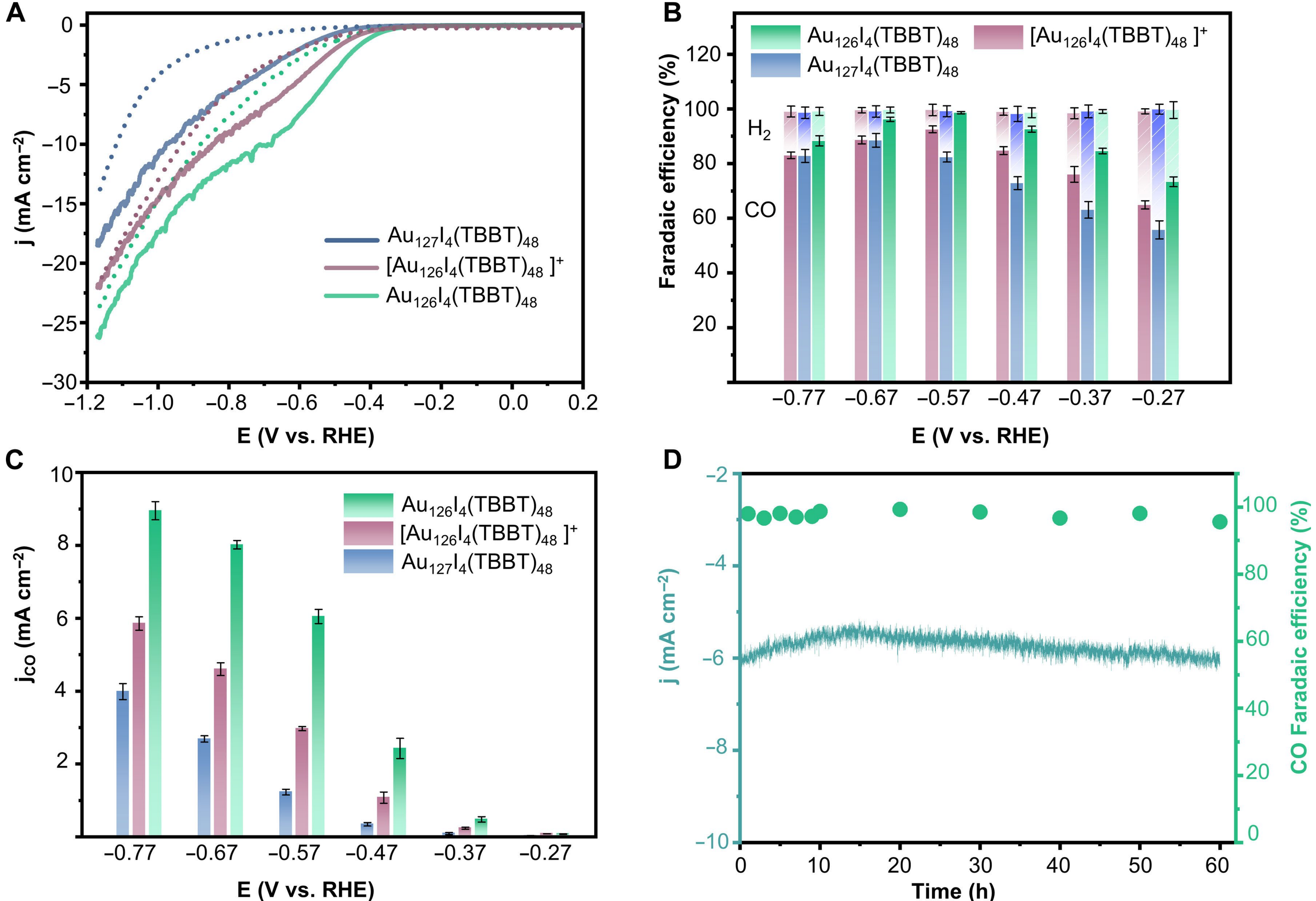

Fig. 5. Electrochemical performance of [Au126]+, Au126, and Au127 nanoclusters.
(A) The LSVs of [Au126]+, Au126, and Au127 nanoclusters in CO2-saturated 0.5 KHCO3 solution with a scan rate of 10 mV s−1. (B) CO Faradaic efficiencies of three nanoclusters for the electrocatalytic reduction of CO2. (C) The corresponding CO partial current densities normalized by the geometrical area of the electrode loaded with separated [Au126]+, Au126, and Au127 nanoclusters. (D) The long-term electrolysis test of Au126 nanoclusters at −0.57 V. h, hours.

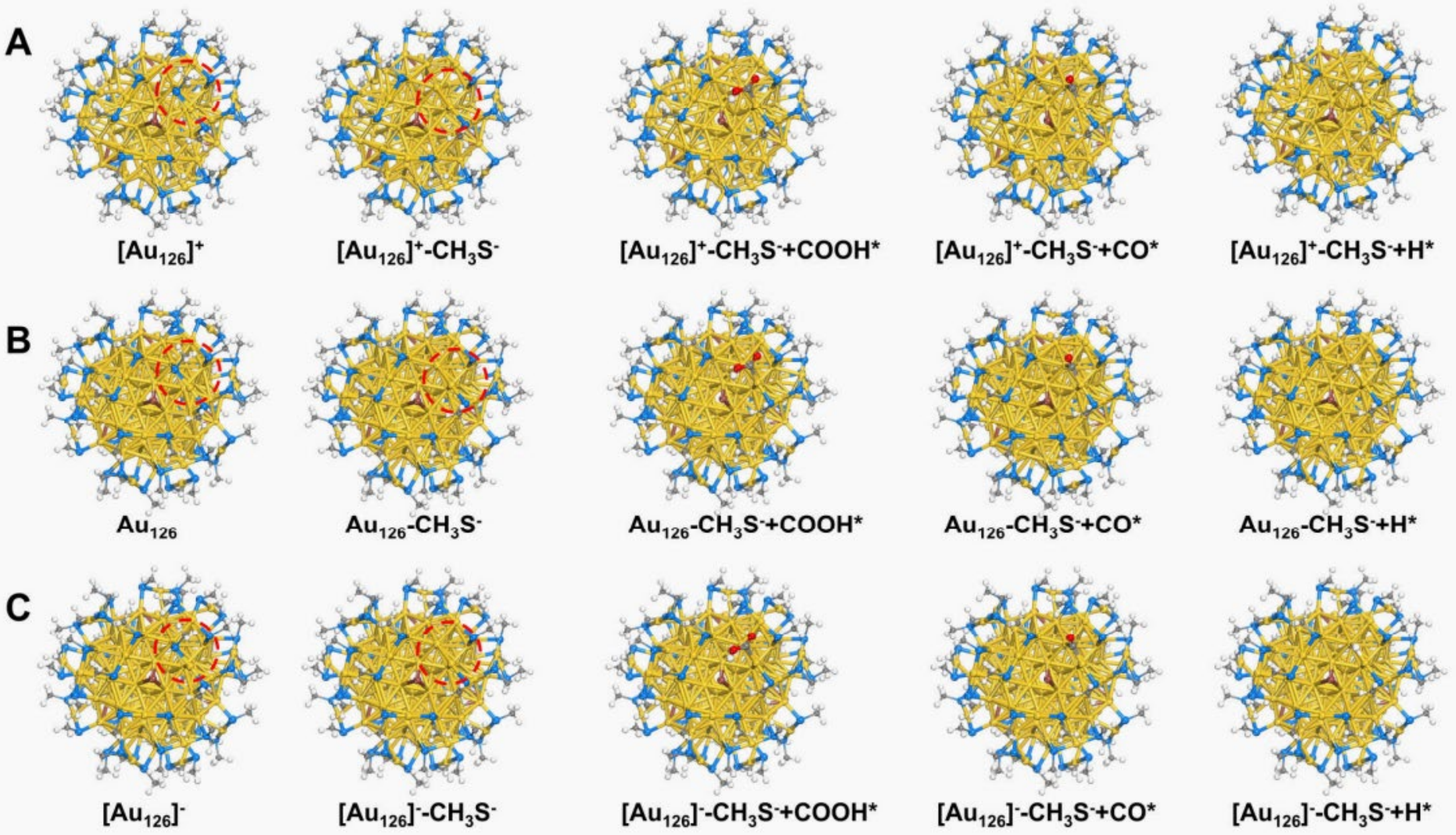

Fig. S32. DFT simulation of the CO_2RR processes for $[Au_{126}]^+$, Au_{126}, and $[Au_{126}]^-$. The optimized structures of active sites (marked with red cycles) on $[Au_{126}I_4(SCH_3)_{48}]^+$ ($[Au_{126}]^+$) and the dethiolated species ($[Au_{126}]^+ - CH_3S^-$), and the corresponding intermediate optimized configurations after adsorbing COOH*, CO*, and H* (**A**); the optimized structures of active sites (marked with red cycles) on $Au_{126}I_4(SCH_3)_{48}$ (Au_{126}) and the dethiolated species ($Au_{126} - CH_3S^-$), and the corresponding intermediate optimized configurations after adsorbing COOH*, CO*, and H* (**B**); and the optimized structures of active sites (marked with red cycles) on $[Au_{126}I_4(SCH_3)_{48}]^-$ ($[Au_{126}]^-$) and the dethiolated species ($[Au_{126}]^- - CH_3S^-$), and the corresponding intermediate optimized configurations after adsorbing COOH*, CO*, and H* $[Au_{126}I_4(SCH_3)_{48}]^-$ (**C**). Color code: Au atoms, yellow;S atoms, green; I atoms, brown; O atoms, red; C atoms, grey; H atoms,white.

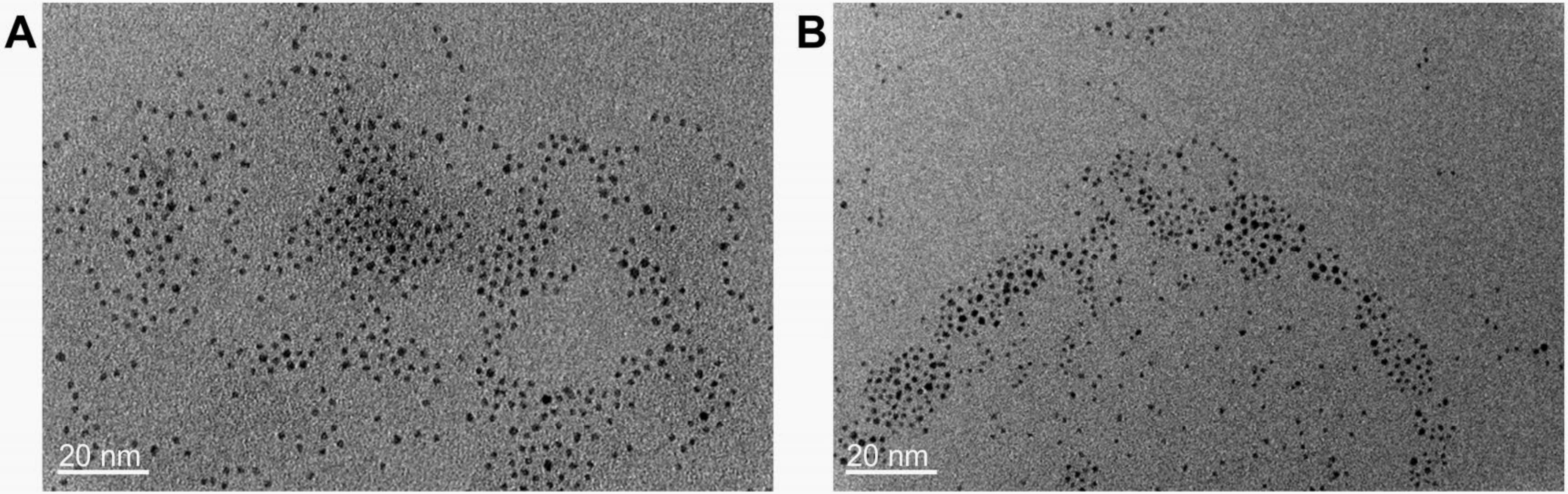

Fig. S34. The TEM images before (A) and after (B) catalysis showed no significant change in particle size of $Au_{126}I_4(TBBT)_{48}$.

But they did not show recyclibility of the catalyst!

Conclusion

- They demonstrated precise, single-atom removal of the innermost gold atom from a large, multi-shell $Au_{127}I_4(TBBT)_{48}$ nanocluster without collapsing the cluster's structural framework.

- This atomic manipulation switches the cluster from paramagnetic (Au_{127}) to diamagnetic (Au_{126}), and further oxidation restores paramagnetism in $[Au_{126}]^+$, enabling consecutive single-atom and single-electron tailoring.

- The removal of the core atom subtly alters the local ligand arrangement, showing that even deep-lying atoms influence surface chemistry and properties (Butterfly Effect).

- The diamagnetic Au_{126} cluster achieves near-unity Faradaic efficiency (~100%) for CO_2-to-CO conversion at low overpotential.